

Active following fuzzy output feedback sliding mode control of real-vehicle semi-active suspensions

H. Liu^{a,*}, K. Nonami^b, T. Hagiwara^c

^a2nd Vehicle Research Dept., Isuzu Advanced Engineering Center, Ltd., 8 Tsuchidana, Fujisawa-shi, Kanagawa-ken, 252-8501, Japan

^bDepartment of Electronics and Mechanical Engineering, Chiba University, 1-33, Yayoi-cho, Inage-ku, Chiba 263-8522, Japan

^cYamaha Motor Co., Ltd., 2500 Shingai, Iwata, Shizuoka 438-8501, Japan

Received 22 August 2007; received in revised form 22 August 2007; accepted 4 January 2008

Handling Editor: L.G. Tham

Available online 4 March 2008

Abstract

Many semi-active suspension systems have been investigated in various literatures in order to achieve lower energy consumption and as good performance as full-active suspension systems. Full-active suspension systems can achieve a good ride quality by actuators; however, their implementation equipments are expensive. The full-active suspensions are perfect from the point of view of control; hence, semi-active control laws with performance similar to full-active controls have attracted the engineering community for their ease and lower cost of implementation. This paper presents a new active following fuzzy output feedback sliding mode control for a real-vehicle semi-active suspension system. The performance of the proposed controller has been verified by comparing it with passive control and also with the full-active target semi-active approximation control method. In the experiment, it was shown that the proposed method has the effectiveness in stabilizing heave, roll and pitch movement of the car body.

© 2008 Elsevier Ltd. All rights reserved.

1. Introduction

To improve the ride quality, the vibrations of a vehicle body should be reduced. In recent years, much attention has been paid to the design of control techniques of the vehicle suspension systems in order to reduce the vibrations. Three types of vibration control methods have been proposed and implemented successfully, namely, the passive, the active and the semi-active method [1]. Passive shock absorbers have fixed damping characteristics determined by their design features. Depending on the road excitation, it is desirable to adjust the characteristics in order to improve the performance of suspension system. Semi-active suspension systems offer the possibility of varying the damper characteristics along with the road profile. The virtues of full-active suspensions versus passive ones have been addressed in many studies [2–5]. In a full-active suspension there are no passive elements such as dampers and springs. The interaction between the vehicle body and a wheel is regulated by an actuator (AC) of variable length. Full-active suspensions have better performance than

*Corresponding author.

E-mail addresses: ryuu-k@iaec.isuzu.co.jp (H. Liu), nonami@faculty.chiba-u.jp (K. Nonami), hagiwarat@yamaha-motor.co.jp (T. Hagiwara).

passive suspensions. However, the active suspension systems are rather complex since they require several components such as ACs, servovalves, high-pressure tanks for the control fluid, sensors for detecting the system, etc. The associated power, which must be provided by the vehicle engine, may be very high depending on the required performance. Furthermore, these suspension systems are very expensive [6]. Semi-active systems can lower the vibration transmission nearly as much as full-active systems without the high cost and power requirements associated with active vibration control systems [7]. Semi-active suspensions have been shown to offer valuable benefits for vehicle suspensions [8–13].

The control strategies of full-active suspension are ideal from the point of view of control. Because of this advantage, the full-active control strategies have been studied in many suspension systems. For example, the ideal sky-hook model following control [14,15] full-active target semi-active approximation control (designs a good active law for a “target” and approximates semi-active control force as close as possible to the target law) [6,8,10,16,17]. However, in the ideal sky-hook model following the control, a single degree-of-freedom suspension model was used so the performance of designed controller was not improved in the high-frequency domain. If the second method is used, the good target active law needs an exact mathematical model. Nevertheless, if the exact mathematical model is used, the active controller will become very complex. Of course, the application of the robust control theory to eliminate the effect of model error exists, for example, the sliding mode control. Needless to say, for the plants that are expressed by linear or nonlinear second-order differential equations, if the matching conditions are satisfied, the sliding model control has strong robustness. However, the estimates of model dynamics and disturbances are very difficult.

In this investigation, we present a new active following fuzzy output feedback sliding mode controller (AFFOSMC), which hybridizes the advantages of the ideal sky-hook model following control and the target active law semi-active control. The basic idea is to improve the semi-active control force, which is derived from the target active law named the output feedback sliding mode control (OSMC) using the fuzzy logic control (FLC) method. Here, the FLC eliminates the tracking error dynamics between the plant and the reference model states. In this paper, the reference model is a semi-active suspension based on target active law (OSMC). The experimental results verify the efficacy of the control strategy.

2. Real vehicle and suspension equipments

The specification of the test vehicle is shown in Table 1. Fig. 1 shows dampers d1–d4 configured to provide adjustable damping for the wheels w1–w4, respectively (the wheels w1 and w3 are hidden). In one configuration, the dampers d1–d4 are electronically controlled dampers. In the other configuration, a stepper motor AC on each damper controls an oil valve. Oil flow in each rotary valve (RV) determines the damping factor provided by the damper.

Fig. 2(a) shows an adjustable damper having an AC that controls a RV. A hard-damping valve (HDV) allows fluid to flow in the adjustable damper to produce hard damping. A soft-damping valve (SDV) allows fluid to flow in the adjustable damper to produce soft damping. The RV controls the amount of fluid that

Table 1
Specification of the test vehicle

Length	4715 mm
Width	1755 mm
Height	1400 mm
Wheel base	2730 mm
Front tread	1485 mm
Rear tread	1495 mm
Capacity	5 persons
Weight	1410 kg
Front suspension	Double wishbone
Rear suspension	Double wishbone
Front tire	195/65R15 91H
Rear tire	195/65R15 91H

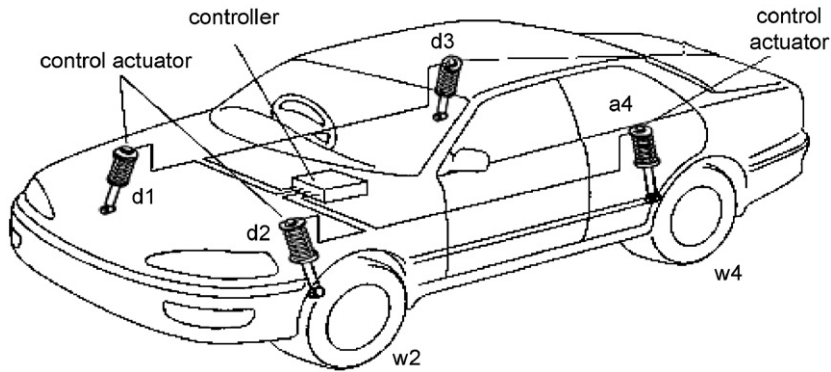


Fig. 1. Suspension system layout of full vehicle.

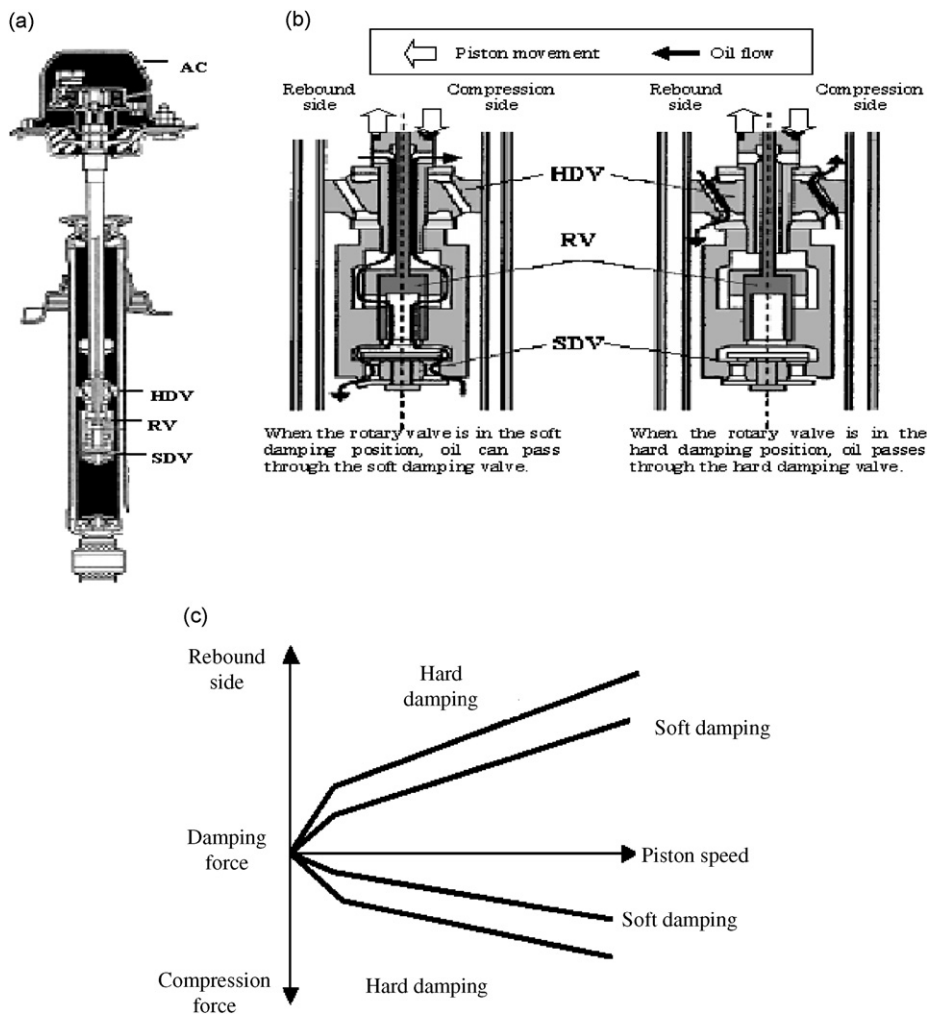


Fig. 2. Characteristics of the variable damper: (a) the external appearance of the damper, (b) oil flow in each rotary position, and (c) damper force characteristics.

flows through the SDV. The AC controls the RV to allow more or less fluid to flow through the SDV, thereby producing a desired damping. In one embodiment, the AC is a stepper motor. The AC receives control signals from the controller shown in Fig. 1. Fig. 2(b) shows fluid flow through the SDV when the RV is

Table 2
Piston velocity vs. damper force

	Speed (m/s)	A (kgf)	B (kgf)	C (kgf)	D (kgf)	E (kgf)
R	1	188.5	197	229.7	297.2	316.7
R	0.5	112.3	115.9	131.3	164.6	174.7
R	0.2	67.3	69.6	81	102.9	110
R	0.1	42.4	43.1	48.7	82.2	89.2
R	0.08	37.4	37.7	41.1	76.9	84.7
R	0.05	28.2	28.3	29.4	54.1	75.9
R	0.03	18.7	18.6	18.8	28.8	58.3
R	0.02	10.5	10.7	10.7	16.1	34.7
R	0.01	4.2	4.3	4.1	5.9	15
C	-0.01	-3.1	-2.7	-2.9	-5.4	-12.4
C	-0.02	-4.1	-3.8	-4.3	-11.4	-16.6
C	-0.03	-5.3	-5	-5.8	-15.6	-19
C	-0.05	-8.6	-8.2	-10.2	-20.2	-22.7
C	-0.08	-15.1	-14.8	-17.7	-25.3	-27.5
C	-0.1	-19.5	-19.2	-21.5	-28.8	-31
C	-0.2	-35.1	-34.6	-36.3	-44.3	-46.4
C	-0.5	-71.5	-71.7	-74.9	-85.7	-89.9
C	-1	-152	-151	-157.9	-180.7	-187.9

opened. Fig. 2(b) also shows fluid flow through the HDV when the RV is closed. Fig. 2(c) shows damper force characteristics as damper force versus piston speed characteristics when the RV is placed in a hard-damping position and in a soft-damping position. The valve is controlled by the stepper motor (the stepper motor with nine steps from the softest position to the hardest position, it takes 7.5 ms to make a step shift), which is placed between the soft and the hard-damping positions to generate intermediate damping force.

Table 2 shows the damper's piston velocity versus the damper force. In the table, "R" stands for rebound and "C" stands for compression. "A" stands for the damper's softest level and "E" stands for the damper's hardest level. From "A" to "E" there are five levels. "Speed" stands for the absolute velocity of the damper.

3. Earlier related works

3.1. Ideal sky-hook model following control

Fig. 3 shows a sky-hook model following sliding mode controller [14,15] for semi-active suspension systems. In this method the basic idea is to force the tracking error dynamics between the plant and the reference model states, instead of the plant dynamics, in the sliding mode so that the plant can physically follow the reference model. However, the drawback of this method is it can only improve the frequency response of the sprung mass in the lower frequency range, without deteriorating the response in the higher frequency range. In a vehicle suspension system, the input of the reference model is the disturbance from the road surface although it cannot be measured. For this reason, the authors had to reduce the degree-of-freedom of the suspension model from two to one. And the inputs of the reference model are position and velocity of the unsprung mass. The sky-hook model following sliding mode controller tried to improve the frequency response of the vehicle at the low-frequency domain, which is closely related to comfort, without deteriorating the frequency response at the high-frequency domain compared to passive suspension systems.

3.2. Full-active target semi-active approximation control

Fig. 4 shows a full-active target semi-active approximation controller [8,16]. There are two steps of this method. First, derive a target active control law that takes the form of a feedback control law. Second, approximate the target law by controlling the damper coefficient of the semi-active suspension. In this method,

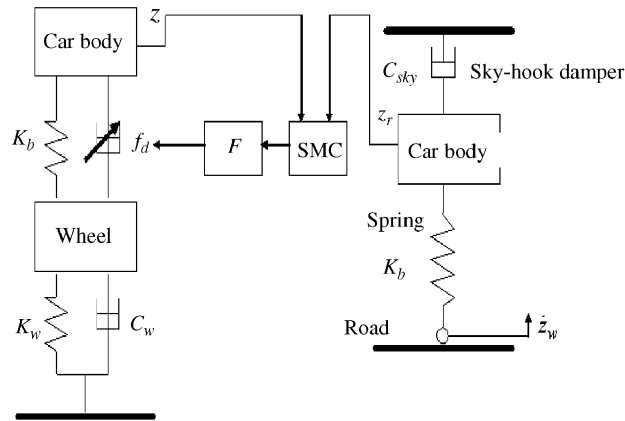


Fig. 3. Sky-hook model following the control scheme.

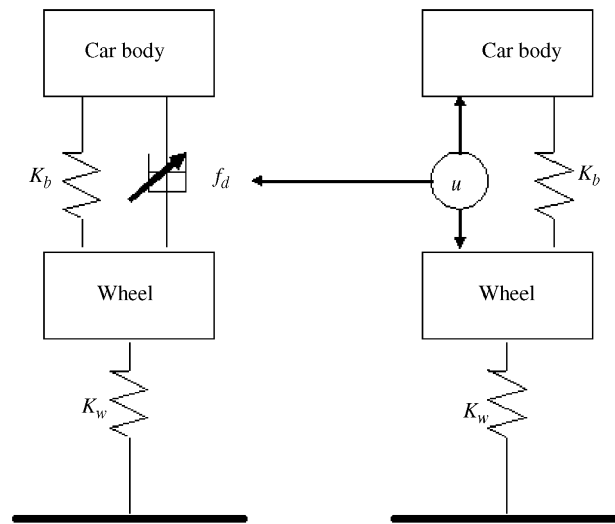


Fig. 4. Full-active target semi-active approximation control scheme.

the good target active control law needs an exact mathematical model. Nevertheless, if using an exact mathematical model the active controller will become very complex. If using a simple mathematical model the error between the mathematical model and the plant cannot be conquered. Of course, the robust control method like SMC can address this problem when the error can be estimated. However, the estimation of the model dynamics is very difficult. For example, the dry friction force of dampers for passenger cars varies widely from 50 to 100 N. The damping coefficient of dampers also deviates by about 10% even when they are brand-new, and deteriorate by more than 10% after several years of use. Change in the weight of the vehicle, from 1500 kg when it is empty to 2000 kg when it is fully loaded with a full tank of fuel and passengers, can cause a shift of 13% in the heave resonance frequency. There are some other nonlinearities caused by rubber bushes and tyres.

The design of the active following fuzzy output feedback sliding mode control to avoid the drawback of an inadequate suspension model will be discussed in the next section. Using OSMC we do not need the input of the reference model (the disturbance of road surface which, cannot be measured) in order to avoid reducing the degree-of-freedom of the suspension model from two to one. Using FLC we can eliminate the error between the two degree-of-freedom suspension model and the real vehicle.

4. Active following fuzzy output feedback sliding mode controller

4.1. Output feedback sliding mode controller

We will design the OSMC system before designing the AFFOSMC system because the target semi-active suspension model is derived from the OSMC system.

Fig. 5 shows the 1/4 semi-active suspension system model. The equations of motion for this model are given by

$$M_b \ddot{z}_b = -K_b(z_b - z_w) - f_c, \tag{1a}$$

$$M_w \ddot{z}_w = K_b(z_b - z_w) + f_c - K_w(z_w - z_r), \tag{1b}$$

where f_c is the damper force output from the damper, and

$$\dot{f}_c = -\frac{1}{T}f_c + \frac{1}{T}\tilde{f}_c, \tag{2a}$$

$$\tilde{f}_c \propto \phi(u, \dot{z}_b - \dot{z}_w), \tag{2b}$$

$$u \propto \phi^{-1}(\tilde{f}_c, \dot{z}_b - \dot{z}_w), \tag{2c}$$

where \tilde{f}_c is the new damper force after T , u is the control input and ϕ is the lookup table.

The state equation for the model is

$$\dot{z} = Az + B_1w + B_2\tilde{f}_c, \tag{3}$$

where $z = [z_b \ \dot{z}_b \ \ddot{z}_b \ z_w \ \dot{z}_w \ \ddot{z}_w]^T$, $w = [z_r \ \dot{z}_r]^T$,

$$A = \begin{bmatrix} 0 & 1 & 0 & 0 & 0 & 0 \\ 0 & 0 & 1 & 0 & 0 & 0 \\ \frac{-K_b}{M_b T} & \frac{-K_b}{M_b} & 0 & \frac{K_b + K_w}{M_b T} & \frac{K_b}{M_b} & \frac{M_w}{M_b T} \\ 0 & 0 & 0 & 0 & 1 & 0 \\ 0 & 0 & 0 & 0 & 0 & 1 \\ \frac{K_b}{M_w T} & \frac{K_b}{M_w} & \frac{M_b}{M_w T} & \frac{-K_b}{M_w T} & \frac{-K_b - K_w}{M_w} & 0 \end{bmatrix}, \quad B_1 = \begin{bmatrix} 0 & 0 \\ 0 & 0 \\ \frac{-K_w}{M_b T} & 0 \\ 0 & 0 \\ 0 & 0 \\ 0 & \frac{K_w}{M_w} \end{bmatrix}, \quad B_2 = \begin{bmatrix} 0 \\ 0 \\ \frac{-1}{M_b T} \\ 0 \\ 0 \\ \frac{1}{M_w T} \end{bmatrix}.$$

Assuming the observation outputs are sprung mass velocity $\dot{z}_b = y_1$ and sprung acceleration $\ddot{z}_b = y_2$, the output equation is given by

$$y = Cz. \tag{4}$$

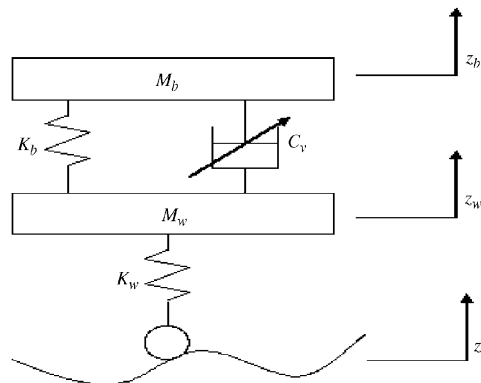


Fig. 5. Quarter car model.

Here,

$$C = \begin{bmatrix} 0 & 1 & 0 & 0 & 0 & 0 \\ 0 & 0 & 1 & 0 & 0 & 0 \end{bmatrix}$$

and

$$\sigma(y) = Sy. \tag{5}$$

Eq. (5) shows the hyper-plane of the OSMC. Here, $S = [h \ 1]$ and Eq. (5) is rewritten as

$$\sigma = hy_1 + y_2, \tag{6}$$

where h is a positive constant and is decided by experiment. Consider a Lyapunov function candidate, $V(\sigma) = \sigma^2/2$, and the following condition:

$$\frac{1}{2} \frac{d}{dt} \sigma^2 = \dot{\sigma}\sigma \leq 0. \tag{7}$$

If Eq. (7) is satisfied, the sliding mode exists.

The following equation is used to satisfy the sliding mode existence condition:

$$\begin{aligned} \sigma(y)\dot{\sigma}(y) &= \sigma SC\dot{z} \\ &= \sigma(SCAz + SCB_1w + SCB_2\tilde{f}_c) < 0. \end{aligned} \tag{8}$$

The design objective is to determine the output feedback control input to satisfy inequality (8). If a matrix $M \in R^{m \times p}$ exists such that

$$SCA = MC \tag{9}$$

then the following relation can be obtained:

$$SCAz = MCz = My. \tag{10}$$

Substituting Eq. (10) into Eq. (8) yields

$$\sigma(y)\dot{\sigma}(y) = \sigma(My + SCB_1w + SCB_2\tilde{f}_c) < 0 \tag{11}$$

and f is given by

$$f = SCB_2\tilde{f}_c. \tag{12}$$

If

$$\begin{aligned} f^+ &< -(My) - SCB_1w, & \sigma(y) > 0, \\ f^- &> -(My) - SCB_1w, & \sigma(y) < 0, \end{aligned} \tag{13}$$

then the sliding mode's existence condition and reaching condition can be satisfied. However, the existence of the matrix M in Eq. (9) is the limitation of this design method. From Eqs. (3), (4) and (6), it can be seen that $SCA \notin \text{Range}(C)$. For this reason, M cannot be solved.

In the case that $SCA = MC$ cannot be resolved, the output feedback control input requires modification. One modification method given in Ref. [18] is

$$\tilde{f}_c = -\mu(SCB_2)^{-1} \frac{\sigma(y)}{\|\sigma(y)\| + \delta}. \tag{14}$$

Here, $\mu > 0$ is the design parameter and δ is a small positive constant for reducing chattering. Substituting Eq. (14) into Eq. (2c) gives

$$\begin{aligned} u &\propto \phi^{-1}(\tilde{f}_c, \dot{z}_b - \dot{z}_w) \\ &\propto \phi^{-1}\left(-\mu(SCB_2)^{-1} \frac{\sigma(y)}{\|\sigma(y)\| + \delta}, \dot{z}_b - \dot{z}_w\right). \end{aligned} \tag{15}$$

From Eq. (15), the OSMC control input can be decided as follows. Firstly, from the relative velocity and Eq. (14) we know that \tilde{f}_c can be computed. Then Table 2 is used to determine the damping level, changing from A to E.

Utilizing the strong robustness of SMC can improve the performance. Nevertheless, the effectiveness is limited because the OSMC system is dependent on the mathematical model. The AFFOSMC is therefore considered to overcome this limitation.

4.2. Active following fuzzy output feedback sliding mode controller

Although the switching controller described above can drive the states trajectories of the reference model to the eventual sliding mode, the error between the reference model and the plant cannot be eliminated. We consider the control as shown in Fig. 6. An additional fuzzy control term u_f is introduced to reduce the error between the reference model and the plant. The fuzzy control term u_f is proposed to have the following form:

$$u_f = -Ke. \tag{16}$$

Here, K is a constant and the error $e = \ddot{z}_b - \ddot{z}_{bp}$.

In order to evaluate riding comfort, we adopted the variable gain K for reducing the error between the acceleration of the car body and the reference model. It is a basic fact that the suspension system performance is sensitive to the parameter K for AFFOSMC applications. For instance, if large values of K are considered then the error between the reference model and the plant will give a fast response, but at the same time, tend to excite chattering. Thus, when the value of e is large, the parameter K should be correspondingly increased. Conversely, if small values of K are chosen, the system chattering will be weak but the system response will become slower. Thus, when the value of e is small, the parameter K should be correspondingly decreased. For this reason, determining the optimum value of K for the system is important. In this investigation, we proposed the parameter K is continuously updated by Fuzzy rules according to the error e , given by

If e is PB, then K is PB.

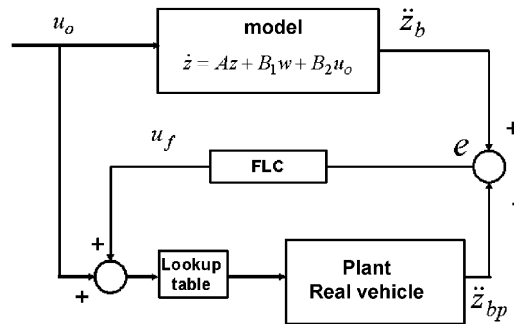


Fig. 6. Active following fuzzy output sliding mode control scheme.

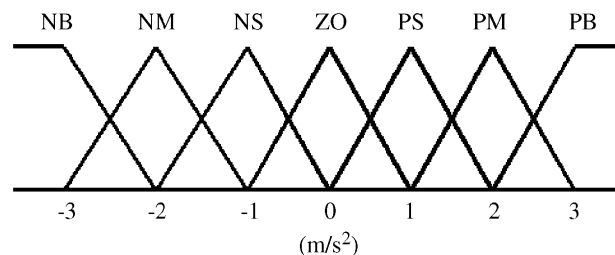


Fig. 7. Membership function of e .

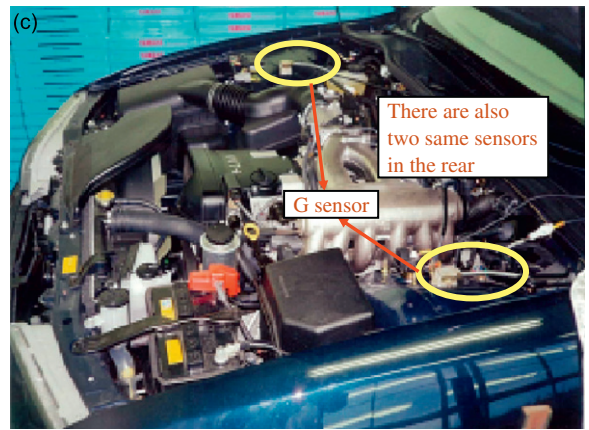
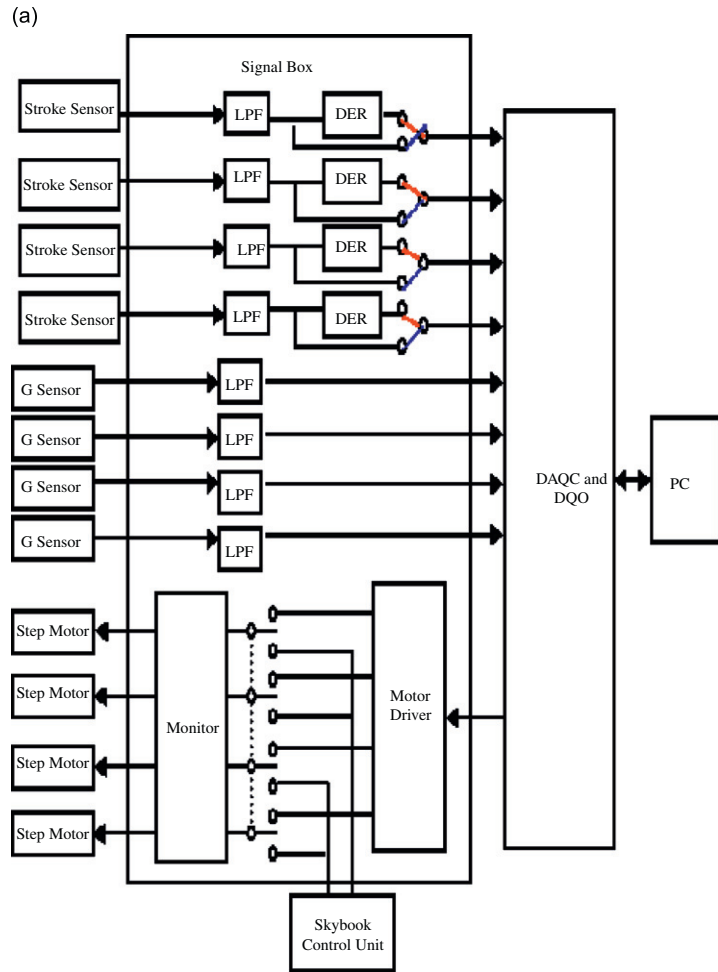


Fig. 8. Experimental system: (a) control system and data acquisition architecture, (b) stroke sensor and (c) G sensor.

Fuzzification of the error e is illustrated in Fig. 7. To conclude the above the discussion, for resolving the drawbacks of the ideal sky-hook model following control and the full-active target semi-active approximation control, the proposed AFFOSM controller is shown as

$$u_{\text{AFFOSMC}} = u_o + u_f, \tag{17}$$

where

$$u_o = \begin{cases} 0 & \text{for } \tilde{f}_c^*(\dot{z}_b - \dot{z}_w) < 0, \\ \text{else } \begin{cases} \tilde{f}_c & \text{if } \tilde{f}_{c\min} \tilde{f}_c < \tilde{f}_{c\max} \\ \tilde{f}_{c\max} & \text{if } \tilde{f}_c > \tilde{f}_{c\max} \text{ or } \tilde{f}_{c\min} \text{ if } \tilde{f}_c < \tilde{f}_{c\min} \end{cases} & \text{for } \tilde{f}_c^*(\dot{z}_b - \dot{z}_w) > 0. \end{cases} \tag{18}$$

5. Experiments

5.1. Experimental setup

The experimental system is shown in Fig. 8. Here, Fig. 8(a) shows the control system and the data acquisition architecture, the stroke sensors shown in Fig. 8(b) measure the stretch and compression position of

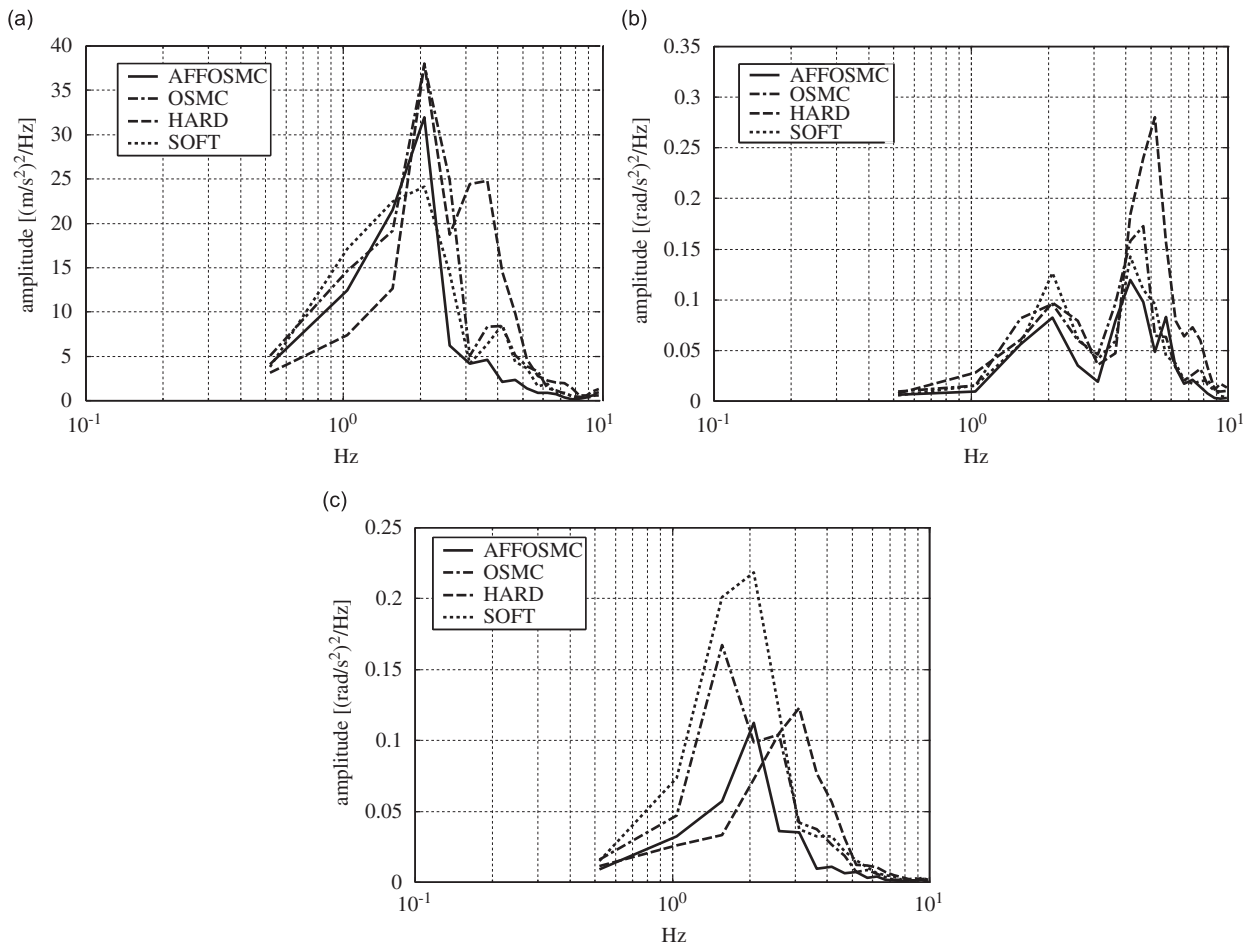


Fig. 9. Response of full vehicle at speed 10k/h: (a) heave response, (b) roll response and (c) pitch response.

the dampers, and the G sensors shown in Fig. 8(c) measure heave acceleration of the car body. DERs differentiate the position signals to speed signals. The LPF blocks are low-pass filters. The acceleration signals and damper relative speed signals pass through the signal box and DAQ Card to the control computer, and the proposed control input is calculated. The control input passes back through the DAQ Card (input/output port between the signal box and the PC) and the signal box to the step motor.

5.2. Results analysis

In order to investigate the performance of the proposed controller, experiments were carried out on the real car. Experimental results without control (passive) are also included for comparison. Figs. 9 and 11 show the comparison of AFFOSMC, OSMC and passive (hard and soft, here hard damping means that the damping coefficient is kept at the maximum position E and soft damping means that the damping coefficient is kept at the minimum position A). The value of the hyper-plane slope h in AFFOSMC and OSMC is the same. Figs. 9 and 11 also show the heave, pitch and roll experimental results. Figs. 10 and 12 show the acceleration results of the reference model and the real vehicle.

Firstly, a suitable hyper-plane slope h from Eq. (6) was decided experimentally. After adjusting the slope h we obtained the switching function σ for each of the 4 corners of the vehicle body. Fig. 9 shows the experimental results at 10 km/h. The experiment was repeated 5 times and the results were averaged to reduce the experimental error. The proposed system performance is sensitive to the sliding surface slope h for OSMC

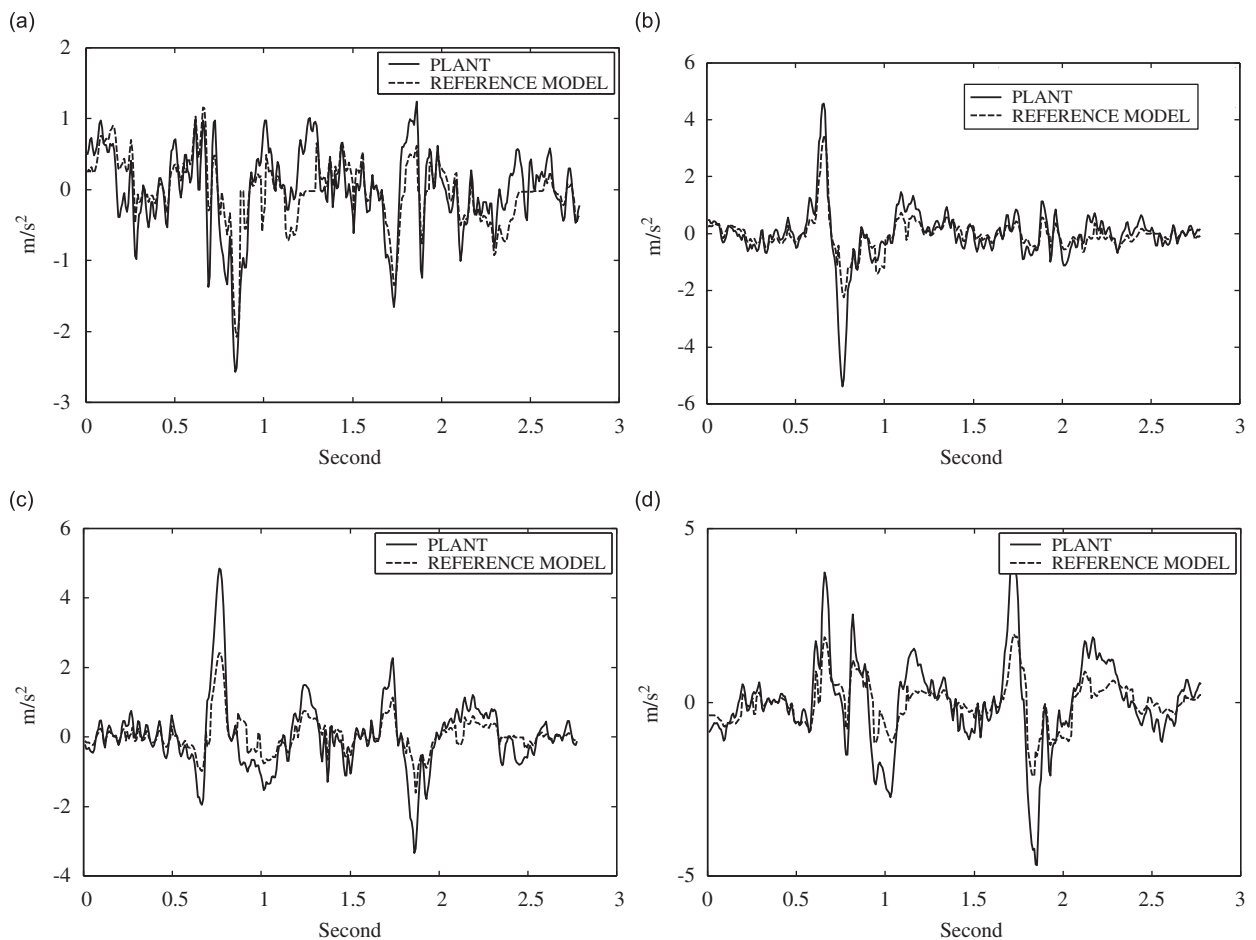


Fig. 10. Experimental results at speed 10 km/h: (a) front left, (b) front right, (c) rear left and (d) rear right.

applications. If “small” values of h are chosen the system will be more stable but the performance may degrade because the control signals will be small and the system response will become slower. If “large” values of h are chosen then the system will respond quickly due to the large values of the control signal but the jerk of the vehicle body becomes more pronounced because the control inputs switch violently. Fig. 9 shows the performance of the AFFOSMC, which is compared with the OSMC and the passive suspensions (hardest and softest damping). The performance of the OSMC is worse than the AFFOSMC because of the limitation of the model error.

Fig. 10 shows the acceleration time history of the vehicle and the reference model at speed 10 km/h. The AFFOSMC controls the four corners of the vehicle body separately, so there are four data. From the figure, we can see that the plant cannot follow the reference model perfectly because of the damper force limitation. It can only follow the reference model globally. Though the plant cannot follow the reference model perfectly, we can see from Fig. 9 that the designed system obtained better performance than the OSMC.

In order to investigate the performance of the AFFOSMC at a different velocity, the experiments were carried out. Fig. 11 shows the experimental results at speed 20 km/h on the same road surface as Fig. 9. Fig. 12 shows the acceleration time history of the vehicle and the reference model, respectively, at speed 20 km/h. From the experimental results we can know that the designed controller also has an excellent performance to isolate disturbance, which comes from the road when the car runs at a different velocity.

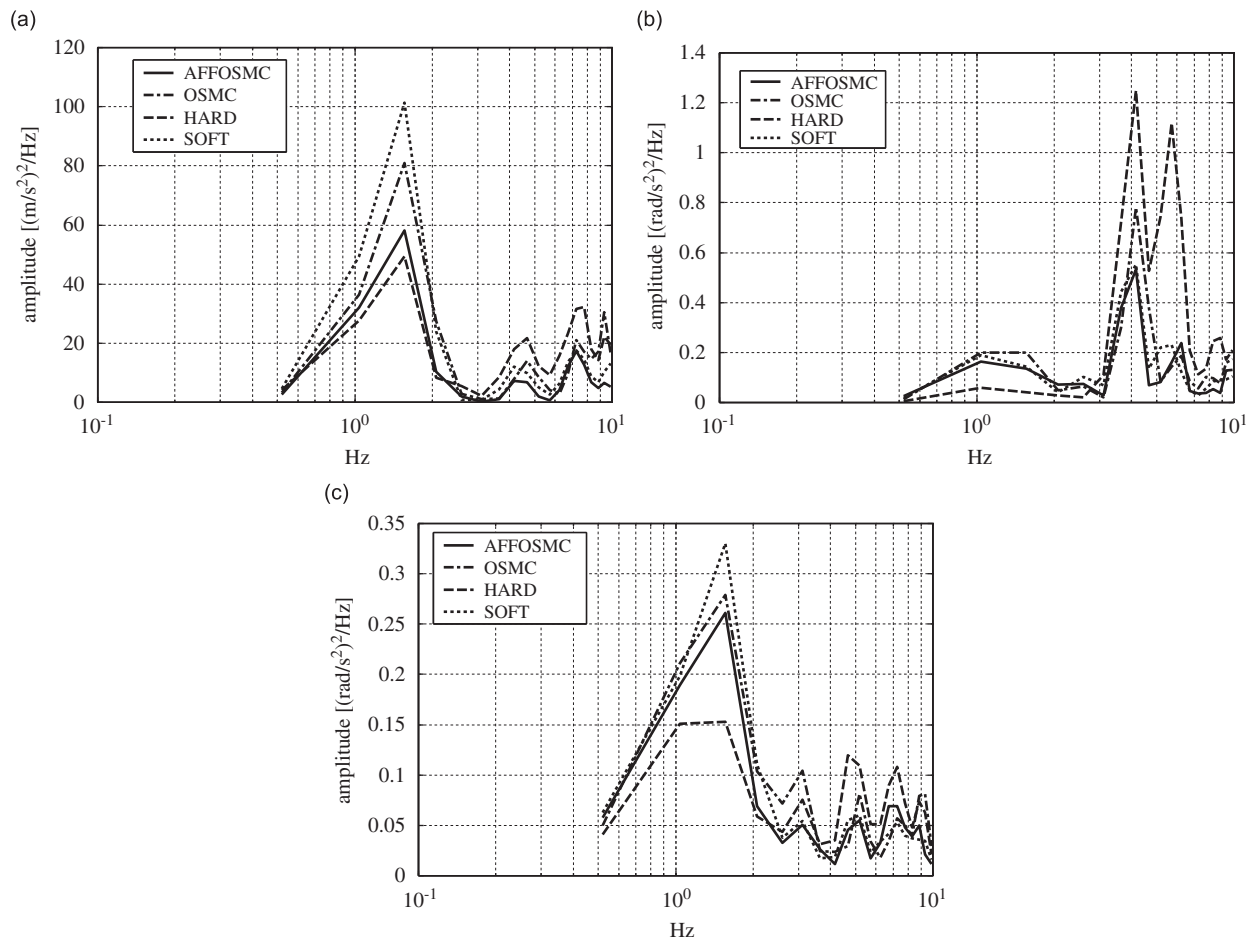


Fig. 11. Response of full vehicle at speed 20 k/h: (a) heave response, (b) roll response and (c) pitch response.

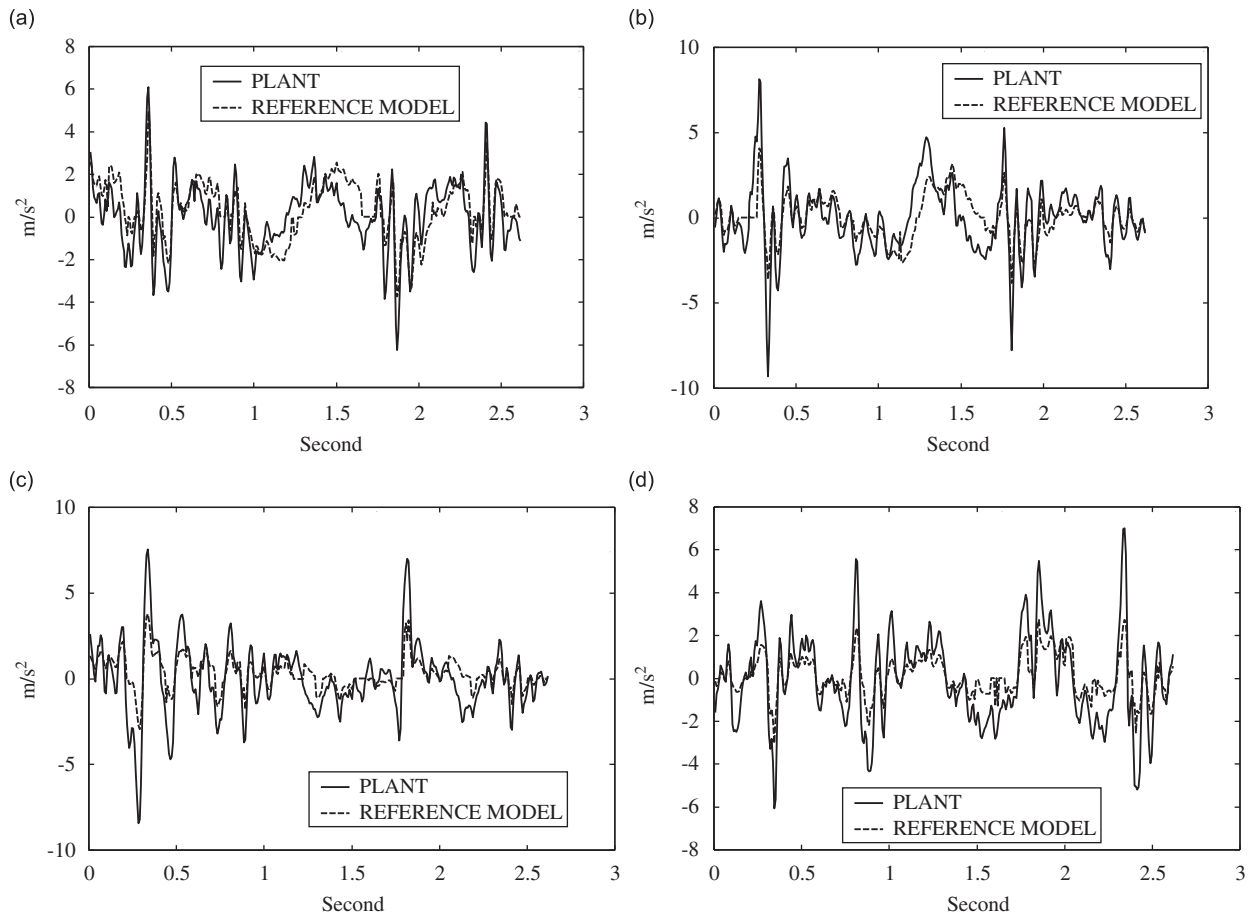


Fig. 12. Experimental results at speed 20 km/h: (a) front left, (b) front right, (c) rear left and (d) rear right.

6. Conclusion

In this paper, a new AFFOSM controller for the real-vehicle semi-active suspension has been investigated. This controller not only derives the semi-active control law from the target active control law but also follows the target active control model. On the basis of the experimental results presented, the following conclusions are drawn:

- (1) The proposed AFFOSM controller avoids the drawbacks of ideal sky-hook model following the controller. It does not need the input of the reference model (the disturbance comes from the road surface, which cannot be measured) so the two degree-of-freedom reference suspension model can be used. The performance of the suspension system at both low- and high-frequency domains can be improved because the degree-of-freedom of the reference suspension model is not reduced from two to one.
- (2) The control input of the full-active target semi-active approximation controller is calculated according to the mathematical suspension model instead of the plant, so its performance is effected by the model error. In order to overcome this drawback, there are two parts in the control input of the proposed controller. The first part is calculated according to the full-active target semi-active approximation control and the second is used for reducing the model error's effect. Its effectiveness has been proved experimentally.
- (3) In fact the plant cannot follow the reference model perfectly, it can only follow the model globally because of the limit of damper force. However, the experimental results suggested that the proposed controller can achieve a high degree of robustness against model error. The proposed AFFOSM controller obtained better performance than the traditional semi-active controller.

References

- [1] T. Sun, Z. Huang, D. Chen, Signal frequency-based semi-active fuzzy control for two-stage vibration isolation system, *Journal of Sound and Vibration* 280 (2005) 965–981.
- [2] U. Stobener, L. Gaul, Active vibration control of a car body based on experimentally evaluated modal parameters, *Mechanical Systems and Signal Processing* 15 (1) (2001) 173–188.
- [3] T. Yoshimura, T. Hiwa, M. Kurimoto, J. Hino, Active suspension system of a one-wheel car model using fuzzy reasoning and compensators, *International Journal of Vehicle Autonomous Systems* 1 (2) (2003) 196–205.
- [4] P. Gaspar, I. Szaszi, J. Bokor, Active suspension design using linear parameter varying control, *International Journal of Vehicle Autonomous Systems* 1 (2) (2003) 206–221.
- [5] T. Yoshimura, K. Watanabe, Active suspension of a full car model using fuzzy reasoning based on single input rule modules with dynamic absorbers, *International Journal of Vehicle Design* 31 (1) (2003) 22–40.
- [6] A. Giua, C. Seatzu, G. Usai, Semi-active suspension design with an optimal gain switching target, *Dynamics and Control* 31 (4) (2000) 213–232.
- [7] X. Song, M. Ahmadian, S. Southward, An adaptive semi-active control algorithm for vehicle suspension systems, *International Mechanical Engineers Conference*, Washington, DC, 2003.
- [8] H. Liu, K. Nonami, Semi-active sliding mode control of full vehicle model and suspensions, *Dynamics & Design Conference*, Nagasaki, 2003, p. 33.
- [9] H. Liu, K. Nonami, T. Hagiwara, Semi-active fuzzy sliding mode control of full vehicle and suspension, *Journal of Vibration and Control* 11 (8) (2005) 1025–1042.
- [10] H. Liu, K. Nonami, T. Hagiwara, Fuzzy sliding mode control of real vehicle semi-active suspensions: comparison with output feedback sliding mode control, *International Journal of Vehicle Autonomous Systems* 3 (2/3/4) (2005) 114–133.
- [11] R. Alkhatib, G. Jazar, Nakhaie, M.F. Golnaraghi, Optimal design of passive linear suspension using genetic algorithm, *Journal of Sound and Vibration* 275 (2004) 665–691.
- [12] S.-J. Heo, K. Park, S.-H. Son, Modelling of continuously variable damper for design of semi-active suspension systems, *International Journal of Vehicle Design* 31 (1) (2003) 41–57.
- [13] S. Yildirim, Vibrations control of suspension systems using a proposed neural network, *Journal of Sound and Vibration* 277 (2004) 1059–1069.
- [14] M. Yokoyama, J.K. Hedrick, S. Yoyama, A model following sliding mode controller for semi-active suspension systems with MR dampers, *Proceedings of the American Control Conference*, Arlington, 2001, pp. 2652–2657.
- [15] M. Yokoyama, J.K. Hedrick, S. Yoyama, A sliding mode controller for semi-active suspension systems, *Transactions of the JSME* 67–657 (C) (2001–2005) 1449–1454.
- [16] A. Giua, M. Melas, C. Seatzu, Design of a control law for a semi-active suspension system using a solenoid valve damper, *Proceedings of the 2004 IEEE Conference on Control Applications*, Taipei, Taiwan, 2004.
- [17] F. Ursu, L. Ursu, Active and semi-active neurocontrollers for suspension systems, 2000. <http://www.incas.ro/romanian/pagini_personale/fursu/fursu.htm#publications>.
- [18] K.Z. Nonami, H.Q. Tian, *Sliding Mode Control Theory*, Korona Press, Tokyo, 1994.